medRxiv preprint doi: https://doi.org/10.1101/2020.04.22.20075804; this version posted April 27, 2020. The copyright holder for this preprint (which was not certified by peer review) is the author/funder, who has granted medRxiv a license to display the preprint in perpetuity. It is made available under a CC-BY-NC-ND 4.0 International license .

Assessing suppression strategies against epidemic outbreaks like COVID-19: the SPQEIR model

Daniele Proverbio[1], Françoise Kemp[1], Stefano Magni[1], Andreas Husch[1], Atte Aalto[1], Laurent Mombaerts[1], Alexander Skupin[1], Jorge Gonçalves[1], Jose Ameijeiras-Alonso[2], and Christophe Ley[3]

[1]University of Luxembourg, Luxembourg Centre for Systems Biomedicine
[2]KU Leuven, Department of Mathematics
[3]Ghent University, Department of Applied Mathematics, Computer Science and Statistics

April 2020

Abstract

The current COVID-19 outbreak represents a most serious challenge for societies worldwide. It is endangering the health of millions of people, and resulting in severe socioeconomic challenges due to lock-down measures. Governments worldwide aim to devise exit strategies to revive the economy while keeping the pandemic under control. The problem is that the effects of distinct measures are not well quantified. This paper compares several suppression approaches and potential exit strategies using a new extended epidemic SEIR model. It concludes that while rapid and strong lock-down is an effective pandemic suppression measure, a combination of other strategies such as social distancing, active protection and removal can achieve similar suppression synergistically. This quantitative understanding will support the establishment of mid- and long-term interventions. Finally, the paper provides an online tool that allows researchers and decision makers to interactively simulate diverse scenarios with our model.

1 Introduction

The current global COVID-19 epidemic has led to significant impairments of public life world-wide. To suppress the spread of the virus and to prevent dramatic situations in the healthcare systems, many countries have implemented rigorous measures for a general lock-down. Evaluation of the epidemic status and forecast of future development is based on statistical methods and on epidemiological models. While statistical methods allow for accurate characterization of the population's health state, epidemiological modeling can provide more detailed mechanisms for the epidemic dynamics and allow investigating how epidemics will develop under different assumptions.
A classical epidemiological model is the SEIR model, that considers individuals transitioning from Susceptible $\rightarrow$ Exposed $\rightarrow$ Infectious $\rightarrow$ Removed state during the epidemics (Anderson and May, 1979). Its essential control parameter is the basic reproduction number R_0 (Legrand et al., 2007). Worldwide general suppression strategies against the current COVID-19 pandemic aim at reducing this quantity. To improve R_0 estimation, this paper develops an extended SEIR model. It incorporates additional compartments reflecting different intervention strategies. In particular, the model focuses on three main suppression programs: social distancing (lowering the rate of social contacts), active protection (lowering the number of susceptible people), and active removal of latent carriers (Anderson et al., 2020). This study investigates how these programs achieve repression both individually and combined. This information can supply Government decisions, helping to avoid overloading the healthcare system and to minimise stressing the economic system (associated with lock-down). We expect our model, together with its interactive online tool, to contribute to crucial tasks of decision making.

NOTE: This preprint reports new research that has not been certified by peer review and should not be used to guide clinical practice.

medRxiv preprint doi: https://doi.org/10.1101/2020.04.22.20075804; this version posted April 27, 2020. The copyright holder for this preprint (which was not certified by peer review) is the author/funder, who has granted medRxiv a license to display the preprint in perpetuity. It is made available under a CC-BY-NC-ND 4.0 International license .

The paper is organized as follows. Section 2 describes the new extended SEIR model. Section 3 presents the main results of our simulations and illustrates the individual and synergetic effects of each suppression measure. A final discussion is provided in Section 4.

2 The SPQEIR Model

2.1 The classical SEIR model

SEIR models are continuous-time, mass conservative compartment-based models of infectious diseases (Anderson and May, 1979; Kermack and McKendrick, 1927). They assume homogeneous propagation media (or fully connected graphs) and focus on the evolution of mean properties of the closed system. Although more realistic versions exist, e.g. SEIR with delay (Yan and Liu, 2006), spatial coupling (Arino et al., 2005), or individual-based models (Ferguson et al., 2006), these models are classical tools to investigate the principal mechanisms governing the spread of infections and their dynamics.
Main compartments of SEIR models (see Fig. 1, framed) are: susceptible S (the pool of individuals likely to be infected), exposed E (corresponding to latent carriers of the infection), infectious I (individuals having developed the disease and being contagious) and removed R (those that have processed the disease, being either recovered or dead). The model's default parameters are the average contact rate β, the inverse of incubation period α, and the average duration of contagious period γ. When focusing on infection dynamics rather than patients' fate, the latter combines recovery and death rate (Noorani, 2010). From these parameters, epidemiologists calculate the "basic reproduction number" $R_0 = \beta/\gamma$ (Fraser et al., 2009) at the epidemic beginning. During the epidemic progression, isolation after diagnosis, vaccination campaigns and active suppression measures are in action. Hence, we speak of "effective reproduction number" $\hat{R}(T))$ being the true fraction of the susceptible population (Althaus, 2014).

2.2 The extended SPQEIR model to reflect suppression strategies

SEIR models reproduce the typical bell-shaped epidemic curves for daily new cases. These quantify the main stressors for both the health system, i.e. the peak π of the curve, and the economic system, i.e. the time $\mathbb{T}$ passed until no new infections occur. Mainstream suppression measures against the epidemic aim at flattening the curve of new infections (Anderson et al., 2020). However, the classical SEIR model is not granular enough to investigate suppression measures, when they need to be considered or should be sequentially reduced if already in place. Therefore, we extend the classical SEIR model as in Fig. 1 (red insertions) into the SPQEIR model. It can be summarized by:

- The classical blocks S, E, I, R are maintained.
- Two new compartments are introduced where
  - Protected P includes individuals that are isolated from the virus and reduces the susceptible pool and
  - Quarantined Q describes latent carriers that are identified and quarantined.

We do not introduce a second quarantined state for isolation of confirmed cases after the Infectious state (Feng, 2007) but consider this together with the Removed state (see Liu et al. (2020b) and references therein). Quarantining infectious symptomatic patients is a necessary first step in every epidemic (Wearing et al., 2005). Notably, the new compartments P (protected) and Q (quarantined) open the classical SEIR closed system by a negative flux out of the original mass-conserving model. An additional link from Q to R, even though realistic, is neglected as both compartments are already outside the "contagion system" and would be therefore redundant from the perspective of infectious evolution. In general, protected individuals can get back to the pool of susceptible after a while, but here we neglect this transition, to focus on simulating repression programs alone. Long-term predictions could be modelled even more realistically by considering such link, that would lead to an additional parameter to be estimated and is beyond the scope of the present paper.

medRxiv preprint doi: https://doi.org/10.1101/2020.04.22.20075804; this version posted April 27, 2020. The copyright holder for this preprint (which was not certified by peer review) is the author/funder, who has granted medRxiv a license to display the preprint in perpetuity. It is made available under a CC-BY-NC-ND 4.0 International license .

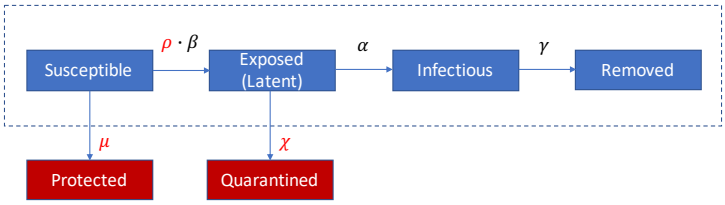

Fig. 1 Scheme of the SPQEIR model. The basic closed SEIR model (framed blue blocks) is extended by the red blocks to the SPQEIR model. Parameters that are linked to repression strategies are shown in red. Interpretation and values of parameters are given in Table 1.

The model has in total 6 parameters. Three of them (β, α, γ in Fig. 1) are based on the classical SEIR model. The new parameters ρ, μ, χ account for alternative repression programs (see Table 1 for details). Commonly, social distancing is modeled by the parameter ρ. It tunes the contact rate parameter β, resulting in the effective reproduction number $\hat{R} = \rho \cdot \beta\gamma^{-1}$. This occurs in a closed-system setting where all individuals belong to the susceptible pool but interact less intensively with each other. The parameter μ stably decreases the susceptible population by introducing an active protection rate. This accounts for improvements of public health, e.g. stricter lock-down of communities, or physical reduction of a country's population like reduced commuters' activity. This changes the effective reproduction number into $\hat{R} = \beta\gamma^{-1}(1-\mu)^T$ with T being the number of days the measures are effective (Peng et al., 2020). The parameter χ introduces an active removal rate of latent carriers. Intensive contact tracing and improved methods to detect asymptomatic latent carriers may enhance the removal of exposed subjects from the infectious network. Following earlier work (Heffernan et al., 2005; Li et al., 1999) and adjusting the current parameters, $\hat{R}$ can be then expressed as $\hat{R} = \beta\gamma^{-1}\alpha\,(\alpha+\chi)^{-1}$. Parameter values that are not related to suppression strategies are taken from recent COVID-19 epidemic literature (Kucharski et al., 2020; Liu et al., 2020b). We use mean values as the main focus of the present model lies on sensitivity analysis of suppression parameters. Our model can be further extended by time dependent parameters or parameters that follow specific distributions (Wearing et al., 2005).
The dynamics of our SPQEIR model are described by the following system of differential equations

$$\begin{aligned}
\dot{\mathrm{S}} &= -\frac{\rho\beta \mathrm{SI}}{N} - \mu \mathrm{S} \\
\dot{\mathrm{E}} &= \frac{\rho\beta \mathrm{SI}}{N} - (\chi+\alpha)\,\mathrm{E} \\
\dot{\mathrm{I}} &= \alpha \mathrm{E} - \gamma \mathrm{I} \\
\dot{\mathrm{R}} &= \gamma \mathrm{I} \\
\dot{\mathrm{P}} &= \mu \mathrm{S} \\
\dot{\mathrm{Q}} &= \chi \mathrm{E}
\end{aligned}$$

with conservation of the total number of individuals, meaning $\dot{\mathrm{N}} = 0$ with N = S + E + I + R + P + Q. As conceptual value, we used N = 10,000. However, N only influences the absolute value of eradication time whereas other results are independent. Overall, the effective reproductive number becomes

$$\hat{R} = \frac{\rho\beta}{\gamma}\frac{\alpha}{\alpha+\chi}(1-\mu)^T, \tag{1}$$

with T being the number of days that the measures leading to compartment P are active.

3 Results

The first three subsections focus on simulation results for single repression programs: social distancing, active protection and active quarantining. Then, we compare a number of synergistic approaches. In particular, we study how crucial quantities, namely the infectious peak height and time to zero infected,

medRxiv preprint doi: https://doi.org/10.1101/2020.04.22.20075804; this version posted April 27, 2020. The copyright holder for this preprint (which was not certified by peer review) is the author/funder, who has granted medRxiv a license to display the preprint in perpetuity. It is made available under a CC-BY-NC-ND 4.0 International license .

Fixed parameters	**Suppression parameters**
R_0 = 2.5	
β = (average contact rate in the population) = 0.85 d^{-1}	μ = (rate of active protection) [d^{-1}]
α = (incubation period)$^{-1}$ = 0.2 d^{-1}	ρ = (social distancing tuning)
γ = (mean infectious period)$^{-1}$ = 0.34 d^{-1} .	χ = (active removal rate) [d^{-1}]

Table 1: SPQEIR model parameters with their standard values from literature (Liu et al., 2020b; Wu et al., 2020). Here "d" stands for days.

depend on suppression parameters and affect $\hat{R}$. We define $\mathbb{T}$ as the time when there are less than 0.5 individuals in the I compartment. This because ODE models approximate discrete quantities with continuous variables.

3.1 Only social distancing

The parameter ρ captures social distancing effects, taking values in the interval $[0, 1]$, where 0 indicates no contacts among individuals while 1 is equivalent to no actions taken. Without loss of generality, simulations consider a delay of 10 days from the first infection to the time social distancing is initiated. Fig. 2 reports simulation results. The infectious curve is progressively flattened by social distancing (2a) and its peak suppressed (2b). However, the eradication time gets delayed for decreasing ρ, until a threshold yielding a disease-free equilibrium rapidly (2c). In this case, the critical value for ρ is 0.4, leading to $\hat{R} < 1$, but $\rho \simeq 0.3$ is more effective in suppressing the epidemic faster.

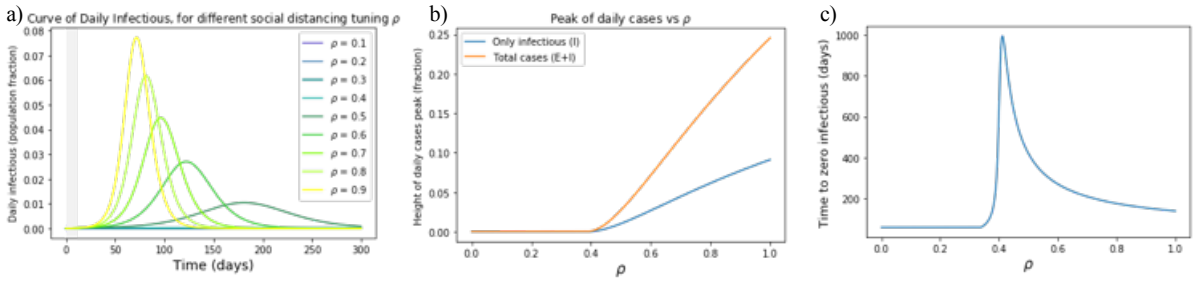

Fig. 2 (a) Effects of social distancing on the epidemic curve. The grey area indicates when measures are not yet in place. (b) The peak π is progressively flattened until a suppression is reached for sufficiently small ρ. For these settings, the critical value for ρ is 0.4 (it pushes $\hat{R}$ below 1). (c) Unless ρ is small enough, stronger measures of this kind might delay the suppression of the epidemic.

3.2 Only active protection

As above, our simulations take into account 10 days delay from the first infection to the initiation of active protection. Range of μ is only up to values similar to those measured in China (Peng et al., 2020). Higher values are considered for step-wise hard lock-down (see below). The results are reported in Fig. 3. We see that small precautions can make an initial difference, but then the effects saturate (Fig. 3a,b). The time to zero infectious is decreased with higher values of active protection (Fig. 3a,b). In particular, $\mu = 0.01\, d^{-1}$ suppresses the epidemics in about 6 months by protecting 70% of the population. Higher values of μ achieve suppression faster, while protecting almost 100% of the population. If protection is mostly achieved through isolation, this is unrealistic. However, this models effective vaccination strategies.

We also consider hard lock-down strategies which isolate many people at once (Liu et al., 2020a). This corresponds to reducing S to a relatively small fraction from one day to the next. Since μ is a rate, we mimic a step-wise hard lock-down by setting a high value to μ but that effect only lasts for a short period of time, see Fig. 4b. In the figure, an example shows how to rapidly protect about 68% of the population

medRxiv preprint doi: https://doi.org/10.1101/2020.04.22.20075804; this version posted April 27, 2020. The copyright holder for this preprint (which was not certified by peer review) is the author/funder, who has granted medRxiv a license to display the preprint in perpetuity. It is made available under a CC-BY-NC-ND 4.0 International license .

with a step-wise μ function. In particular, we use a two-days long step-wise μ function (Fig. 4b) to mimic the rapid, but not abrupt, change in mobility observed in many countries by Google Mobility Reports (Google, 2020). Lock-down effects are reported in Fig. 4: a hard lock-down is effective in suppressing the epidemic curve and in lowering the eradication time (as shown by the Chinese experience).

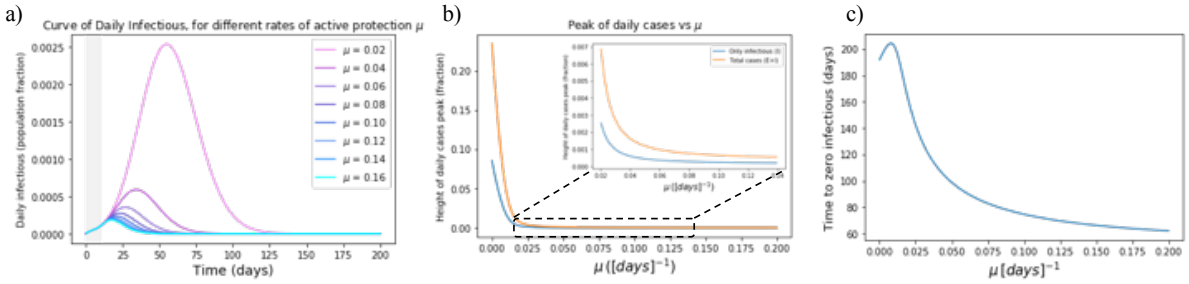

Fig. 3 (a) Effects of active protection on the infectious curve. The grey area indicates when measures are not yet in place. μ units is d^{-1} (b) Dependency of peak height on μ: the peak is rapidly flattened for increasing μ, then it is smoothly reduced for higher parameter values. (c) High μ values are effective in anticipating the complete eradication of the epidemic, but require protecting more than 90% of the population.

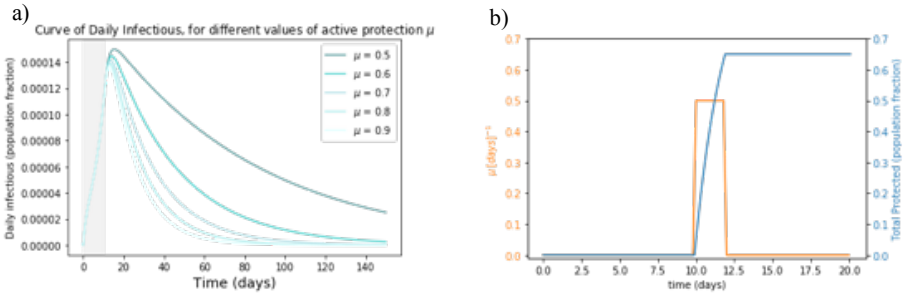

Fig. 4 (a) Flattening the infectious curve by hard lock-down. Rapidly isolating a large population fraction is effective in suppressing the epidemic spreading. (b) Modeling hard lock-down: high μ (orange) is active for two days to isolate and protect a large population fraction rapidly (blue). As an example, we show $\mu = 0.5\, d^{-1}$ if $t \in [10, 12]$. It results in protecting about 68% of the population in two days. Another example, $\mu = 0.9\, d^{-1}$ would protect 86% of the population at once.

3.3 Only active quarantining

The simulations in this part are based on realistic assumptions: testing a person is effective only after a few days that person has been exposed (to have a viral charge that is detectable). It induces a maximal quarantining rate θ, which we set $\theta = 0.33\, d^{-1}$ as testing is often considered effective after about 3 days from contagion (Corman et al., 2020). Therefore, we get the active quarantining rate $\chi = \chi' \cdot \theta$, where χ' is a tuning parameter associated e.g. to contact tracing. As θ is fixed, we focus our analysis on χ'. As above, we also assume that testing starts after the epidemic is seen in the population, e.g. some infectious are identified. This induces the usual 10 days delay in the activation of measures.
The corresponding results are reported in Fig. 5. The curve is progressively flattened by latent carriers quarantining and its peak suppressed, but the eradication time gets delayed for increasing χ'. This happens until a threshold value of $\chi'_{thr} = 0.9$ that pushes $\hat{R}$ below 1. This value holds if we accept a strategy based on testing, with $\theta = 0.33$. If preventive quarantine of suspected cases does not need testing (for instance, it is achieved by contact tracing apps), the critical χ' value could be drastically lower. In particular, $\chi'_{thr} = 0.3\, d^{-1}$ if $\theta = 1\, d^{-1}$, i.e. latent carriers are quarantined the day after a contact.

medRxiv preprint doi: https://doi.org/10.1101/2020.04.22.20075804; this version posted April 27, 2020. The copyright holder for this preprint (which was not certified by peer review) is the author/funder, who has granted medRxiv a license to display the preprint in perpetuity. It is made available under a CC-BY-NC-ND 4.0 International license .

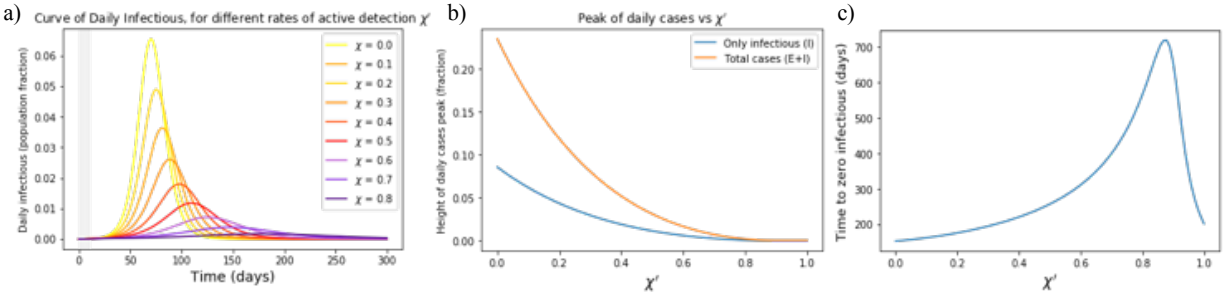

Fig. 5 (a) Effects of active latent carriers quarantining on the epidemic curve. The grey area indicates when measures are not yet in place. (b) The peak is progressively flattened until a disease-free equilibrium is reached for sufficiently large χ. (c) Unless χ' is large enough, stronger measures of this kind might delay the complete eradication of the epidemic. Note that the critical χ' can be lowered for higher θ, e.g. if preventive quarantine does not wait for a positive test.

The parameter χ' tunes the rate of removing latent carriers. Hence, it combines tracing and testing capacities, i.e. probability of finding latent carriers (P_{find}) and probability that their tests are positive (P_+). The latter depends on the false negative rate δ_- as

$$P_+ = (1 - \delta_-)\,. \tag{2}$$

So, $\chi' = P_{find} \cdot P_+$. Hence, suppressing the infectious peak requires an adequate balance of accurate tests and good tracing success as reported in Fig. 6. Further quantifying the latter would drastically improve our understanding of the current capabilities and of bottlenecks, towards a more comprehensive feasibility analysis.

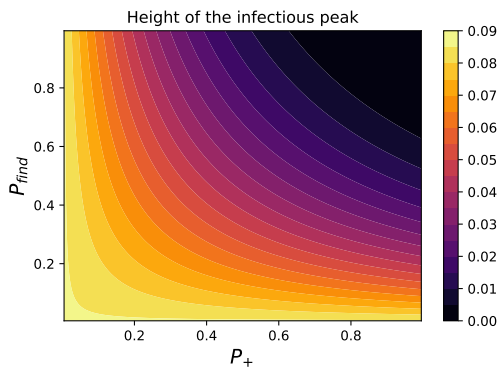

Fig. 6 Assessing the impact of P_{find} and P_+ on the infectious peak separately. This way, we separate the contribution of those factors to look at resources needed from different fields, e.g. network engineering or wet lab biology. Solutions to boost the testing capacity like (Hanel and Thurner, 2020) could impact both terms.

3.4 Synergistic approaches

Fully enhanced active quarantining and active protection might not be always feasible, e.g. because of limited resources, technological limitations or welfare restrictions. Therefore a synergistic approach is very attractive as it can flatten the curve. This section shows a number of possible synergies, concentrating as before on abstract scenarios to investigate the effect of combining different suppression programs. As case studies, we consider the 6 synergistic scenarios listed below. Parameters are set without being specific to real measures taken: their value is so far conceptual and meaningful when compared across scenarios. Just like above, we consider a 10 days delay from the first infection to issuing measures; as suggested in other studies (Deutsche Gesellschaft für Epidemiologie, 2020), delaying action could

medRxiv preprint doi: https://doi.org/10.1101/2020.04.22.20075804; this version posted April 27, 2020. The copyright holder for this preprint (which was not certified by peer review) is the author/funder, who has granted medRxiv a license to display the preprint in perpetuity. It is made available under a CC-BY-NC-ND 4.0 International license .

worsen the situation. To differentiate between a rapid isolation and a constant protection, we introduce μ_{ld} (for "hard lock-down strategies", see Section 3.2) separate from μ. To get $\hat{R}$, we follow Eq. 1, considering $\chi = \chi' \cdot \theta$ as in Section 3.3 and $T = 30$ (along the steep decay after measures are in place). Our scenarios are the following:

1. Many European countries opted for a lock-down strategy. A quite large fraction of the population was isolated, individuals were recommended to self-quarantine in case of suspected positiveness, social distancing got mandatory but was sometimes not fully followed, masks and sprays were suggested for protection. So, we set an initial "hard lock-down" $\mu_{ld} = 0.2\, d^{-1}$ to protect around 35% of the population quickly. Then we chose $\rho = 0.7$, $\chi' = 0.15$ and $\mu = 0.008\, d^{-1}$. This yields $\hat{R} = 0.7$.

2. An alternative procedure is to rapidly protect only the population fraction at high risk ($\mu_{ld} = 0.06\, d^{-1}$, letting 15% of initial S to P). Then, we assume an improvement in individual safety giving $\mu = 0.01\, d^{-1}$. Social distancing is relaxed ($\rho = 0.8$) but latent carrier quarantine is enforced ($\chi' = 0.5$). This gives $\hat{R} = 0.7$.

3. In case preventive quarantine of latent carriers is not greatly effective ($\chi' = 0.1$), and in case of low protection rate and scarce isolation ($\mu = 0.004\, d^{-1}$, $\mu_{ld} = 0.1\, d^{-1}$), we rise social distancing for all individuals doing business as usual ($\rho = 0.5$). In this case, $\hat{R} = 0.7$.

4. If there are no safety devices that provide an adequate protection ($\mu = 0\, d^{-1}$), we set $\rho = 0.45$, $\mu_{ld} = 0.2\, d^{-1}$ and $\chi' = 0.2$ to get $\hat{R} = 0.7$.

5. This case has higher $\hat{R}$ than the previous ones, namely $\hat{R} = 0.9$. The corresponding parameters are $\mu_{ld} = 0.2\, d^{-1}$, $\mu = 0.002\, d^{-1}$, $\rho = 0.7$, $\chi' = 0.1$.

6. Finally, we consider "draconian" measures such that $\hat{R} = 0.3$ only through isolation and massive latent carriers quarantining. So, $\mu_{ld} = 0.6\, d^{-1}$ and $\chi' = 0.3$ while $\rho = 1$ and $\mu = 0\, d^{-1}$.

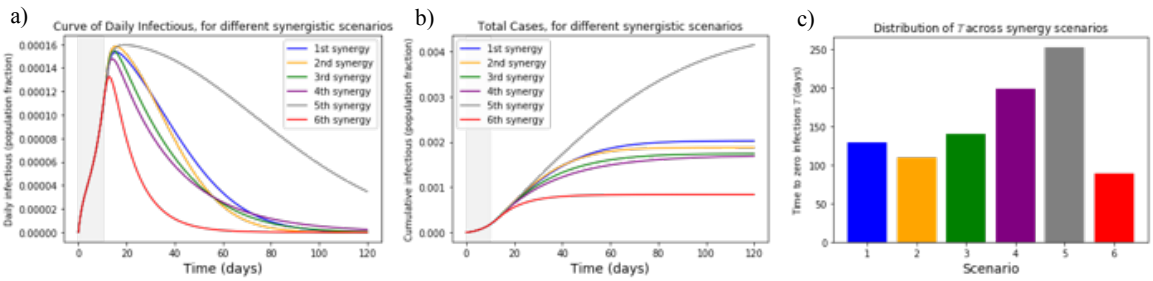

Fig. 7 Simulations of the 6 synergistic scenarios. (a) New cases curves, (b) Cumulative cases. The grey area indicates when measures are not yet in place. It is evident that scenarios leading to the same $\hat{R}$ could show different patterns and suppression timing. (c) Distribution of times to zero infections $\mathbb{T}$ for different scenarios.

Simulation results are reported in Fig. 7. Different synergies lead to different timing, even though the peak is contained similarly (Fig. 7a). This has an impact on the cumulative number of cases (Fig. 7b) that will be reflected on the death toll. This holds even when the $\hat{R}$ values are very close, as in scenarios 1 to 4. Focusing on scenarios 2 and 3, we notice that prevention measures and latents quarantine accelerate the suppression, even when isolating only vulnerable people. This achieves similar effects as strong social distancing. In addition, active protective measures with relatively low values further concur in suppressing the peak. This finding asks for rapid assessment of masks and sanitising routines.
Overall, the strength of suppression measures influences how and how fast the epidemic is flattened. An $\hat{R} < 1$ suffices to avoid breakdown of the health system, but its effects could be too slow for the economic system. Decreasing its value with synergistic interventions could speed up epidemic suppression. Given the importance of magnitudes in achieving suppression, it is hardly conceivable to transfer

medRxiv preprint doi: https://doi.org/10.1101/2020.04.22.20075804; this version posted April 27, 2020. The copyright holder for this preprint (which was not certified by peer review) is the author/funder, who has granted medRxiv a license to display the preprint in perpetuity. It is made available under a CC-BY-NC-ND 4.0 International license .

directly results across countries when attempting data fitting: even though the peak suppression can be reproduced, epidemic eradication might have different timing. A careful assessment of measures' strength is thus recommended for cross-country comparison.

4 Discussion

We have developed a conceptual model to assess non-pharmaceutical suppression strategies on top of social distancing. They have different effects on epidemic evolution in terms of curve flattening and eradication timing. As with previous studies (Ferguson et al., 2020; Peak et al., 2020), we have observed the need to enforce mitigation measures (i.e., slow down viral spread in the community with social distancing) along with containment (i.e., detect and isolate cases, identify and quarantine contacts and at risk neighborhoods).

By extending the classic SEIR model into the SPQEIR model, we distinguished the impact of different repression programs in flattening the peak and anticipating the eradication of the epidemic. Depending on their strength and synergy, non-pharmaceutical interventions can hamper the disease from spreading in a population. It is now necessary to move from idealised representations to realistic scenarios and to map policy measures to abstract programs. This will require ad-hoc or post-hoc quantification of specific interventions, e.g. how effective masks are in protecting people, how much proximity tracing apps increase P_{find}, how changes in behavior are associated with epidemic decline (Cowling et al., 2020) and so on. Some real measures might also affect multiple parameters at once, e.g. safety devices and lock-down could impact both μ and ρ. Their assessment is demanded to close discussions between modelers and experts of public hygiene. We also acknowledge that practical implementations have to consider available resources in crisis periods. A word of caution: the present model aims at informing researchers and policy-makers by examining possible abstract scenarios and comparing quantitative, model-based outputs. It is not intended to faithfully represent specific countries nor to fully reproduce the epidemic complexity within societies. Any conclusion should be carefully interpreted by experts, and the feasibility of tested scenarios should be discussed before reaching consensus.

Overall, this work could contribute to quantitative assessments of epidemic repression strategies. To tackle the current epidemic wave, and against possible resurgence of contagion (Kissler et al., 2020), better understanding the effect of different non-pharmaceutical interventions could help planning mid- and long-term measures towards phase 2, until a vaccine is available.

Shinyapp

A user-friendly online shinyapp to interactively simulate different scenarios is available on: `https://jose-ameijeiras.shinyapps.io/SPQEIR_model/`. It allows to reproduce the present outputs and to perform sensitivity analysis.

Code for analysis

The code is publicly available on github at: `https://github.com/daniele-proverbio/Covid-19`.

Acknowledgements

Fundings: DP and SM's work is supported by the FNR PRIDE DTU CriTiCS, ref 10907093. FK's work is supported by the Luxembourg National Research Fund PRIDE17/12244779/PARK-QC. A.H. work was partially supported by the Fondation Cancer Luxembourg. JG is partly supported by the 111 Project on Computational Intelligence and Intelligent Control, ref B18024. AA is supported by the Luxembourg National Research Fund (FNR) (Project code: 13684479). JAA is supported by the FWO research project G.0826.15N (Flemish Science Foundation), GOA/12/014 project (Research Fund KU Leuven), Project MTM2016-76969-P from the Spanish State Research Agency (AEI) co–funded by the European Regional

medRxiv preprint doi: https://doi.org/10.1101/2020.04.22.20075804; this version posted April 27, 2020. The copyright holder for this preprint (which was not certified by peer review) is the author/funder, who has granted medRxiv a license to display the preprint in perpetuity. It is made available under a CC-BY-NC-ND 4.0 International license .

Development Fund (ERDF) and the Competitive Reference Groups 2017–2020 (ED431C 2017/38) from the Xunta de Galicia through the ERDF.

Declaration of competing interest

The authors declare no competing interests.

Contributors

DP, AH designed the study. DP, FK, SM developed the model. DP, FK, JAA implemented the model. DP, FK, SM, AH, AA, LM, AS, JG, CL analyzed and interpreted the results. SM, AH, AS, JG, CL supervised and coordinated the project. DP, FK, SM, CL wrote the first draft. All authors contributed to the final draft. All authors gave their final approval for publication.

References

Althaus, C. L. (2014). Estimating the reproduction number of Ebola virus (EBOV) during the 2014 outbreak in West Africa. *PLoS Currents*, 6.

Anderson, R. M., Heesterbeek, H., Klinkenberg, D., and Hollingsworth, T. D. (2020). How will country-based mitigation measures influence the course of the COVID-19 epidemic? *The Lancet*, 395(10228):931–934.

Anderson, R. M. and May, R. M. (1979). Population biology of infectious diseases: Part I. *Nature*, 280(5721):361–367.

Arino, J., Davis, J. R., Hartley, D., Jordan, R., Miller, J. M., and Van Den Driessche, P. (2005). A multi-species epidemic model with spatial dynamics. *Mathematical Medicine and Biology*, 22(2):129–142.

Corman, V. M., Landt, O., Kaiser, M., Molenkamp, R., Meijer, A., Chu, D. K., Bleicker, T., Brünink, S., Schneider, J., Schmidt, M. L., et al. (2020). Detection of 2019 novel coronavirus (2019-nCoV) by real-time RT-PCR. *Eurosurveillance*, 25(3):2000045.

Cowling, B. J., Ali, S. T., Ng, T. W., Tsang, T. K., Li, J. C., Fong, M. W., Liao, Q., Kwan, M. Y., Lee, S. L., Chiu, S. S., et al. (2020). Impact assessment of non-pharmaceutical interventions against coronavirus disease 2019 and influenza in hong kong: an observational study. *The Lancet Public Health*.

Deutsche Gesellschaft für Epidemiologie (2020). Stellungnahme der Deutschen Gesellschaft für Epidemiologie (DGEpi) zur Verbreitung des neuen Coronavirus (SARS-CoV-2). *www.dgepi.de*.

Feng, Z. (2007). Final and peak epidemic sizes for SEIR models with quarantine and isolation. *Mathematical Biosciences & Engineering*, 4(4):675.

Ferguson, N. M., Cummings, D. A., Fraser, C., Cajka, J. C., Cooley, P. C., and Burke, D. S. (2006). Strategies for mitigating an influenza pandemic. *Nature*, 442(7101):448–452.

Ferguson, N. M., Laydon, D., Nedjati-Gilani, G., Imai, N., Ainslie, K., Baguelin, M., Bhatia, S., Boonyasiri, A., Cucunubá, Z., Cuomo-Dannenburg, G., et al. (2020). Impact of non-pharmaceutical interventions (NPIs) to reduce COVID-19 mortality and healthcare demand. *Imperial College, London. DOI: https://doi. org/10.25561/77482*.

Fraser, C., Donnelly, C. A., Cauchemez, S., Hanage, W. P., Van Kerkhove, M. D., Hollingsworth, T. D., Griffin, J., Baggaley, R. F., Jenkins, H. E., Lyons, E. J., et al. (2009). Pandemic potential of a strain of influenza A (H1N1): early findings. *Science*, 324(5934):1557–1561.

Google (2020). COVID-19 Community Mobility Reports. *https://www.google.com/covid19/mobility/*.

medRxiv preprint doi: https://doi.org/10.1101/2020.04.22.20075804; this version posted April 27, 2020. The copyright holder for this preprint (which was not certified by peer review) is the author/funder, who has granted medRxiv a license to display the preprint in perpetuity. It is made available under a CC-BY-NC-ND 4.0 International license .

Hanel, R. and Thurner, S. (2020). Boosting test-efficiency by pooled testing strategies for SARS-CoV-2. *arXiv preprint arXiv:2003.09944*.

Heffernan, J. M., Smith, R. J., and Wahl, L. M. (2005). Perspectives on the basic reproductive ratio. *Journal of the Royal Society Interface*, 2(4):281–293.

Kermack, W. O. and McKendrick, A. G. (1927). A contribution to the mathematical theory of epidemics. *Proceedings of the royal society of london. Series A, Containing papers of a mathematical and physical character*, 115(772):700–721.

Kissler, S. M., Tedijanto, C., Goldstein, E., Grad, Y. H., and Lipsitch, M. (2020). Projecting the transmission dynamics of SARS-CoV-2 through the postpandemic period. *Science*.

Kucharski, A., Russell, T., Diamond, C., and Liu, Y. (2020). Analysis and projections of transmission dynamics of nCoV in Wuhan. *CMMID repository*, 2.

Legrand, J., Grais, R. F., Boelle, P.-Y., Valleron, A.-J., and Flahault, A. (2007). Understanding the dynamics of Ebola epidemics. *Epidemiology & Infection*, 135(4):610–621.

Li, M. Y., Graef, J. R., Wang, L., and Karsai, J. (1999). Global dynamics of a SEIR model with varying total population size. *Mathematical biosciences*, 160(2):191–213.

Liu, X., Hewings, G. J., Qin, M., Xiang, X., Zheng, S., Li, X., and Wang, S. (2020a). Modelling the situation of COVID-19 and effects of different containment strategies in China with dynamic differential equations and parameters estimation. *Available at SSRN 3551359*.

Liu, Y., Gayle, A. A., Wilder-Smith, A., and Rocklöv, J. (2020b). The reproductive number of COVID-19 is higher compared to SARS coronavirus. *Journal of Travel Medicine*.

Noorani, M. (2010). SEIR model for transmission of dengue fever in Selangor Malaysia. In *International Journal of Modern Physics: Conference Series*, volume 1, pages 1–5.

Peak, C. M., Kahn, R., Grad, Y. H., Childs, L. M., Li, R., Lipsitch, M., and Buckee, C. O. (2020). Modeling the Comparative Impact of Individual Quarantine vs. Active Monitoring of Contacts for the Mitigation of COVID-19. *medRxiv*.

Peng, L., Yang, W., Zhang, D., Zhuge, C., and Hong, L. (2020). Epidemic analysis of COVID-19 in China by dynamical modeling. *arXiv preprint arXiv:2002.06563*.

Wearing, H. J., Rohani, P., and Keeling, M. J. (2005). Appropriate models for the management of infectious diseases. *PLoS medicine*, 2(7).

Wu, J. T., Leung, K., and Leung, G. M. (2020). Nowcasting and forecasting the potential domestic and international spread of the 2019-nCoV outbreak originating in Wuhan, China: a modelling study. *The Lancet*, 395(10225):689–697.

Yan, P. and Liu, S. (2006). SEIR epidemic model with delay. *The ANZIAM Journal*, 48(1):119–134.